Cdk5rap2 regulates centrosome function and chromosome segregation in neuronal progenitors

Sofia B. Lizarraga[1], Steven P. Margossian[2,3], Marian H. Harris[2,4], Dean R. Campagna[2], An-Ping Han[2], Sherika Blevins[2], Raksha Mudbhary[1,*], Jane E. Barker[5], Christopher A. Walsh[1,†] and Mark D. Fleming[2,†]

SUMMARY

Microcephaly affects ~1% of the population and is associated with mental retardation, motor defects and, in some cases, seizures. We analyzed the mechanisms underlying brain size determination in a mouse model of human microcephaly. The *Hertwig's anemia* (*an*) mutant shows peripheral blood cytopenias, spontaneous aneuploidy and a predisposition to hematopoietic tumors. We found that the *an* mutation is a genomic inversion of exon 4 of *Cdk5rap2*, resulting in an in-frame deletion of exon 4 from the mRNA. The finding that *CDK5RAP2* human mutations cause microcephaly prompted further analysis of *Cdk5rap2^an/an^* mice and we demonstrated that these mice exhibit microcephaly comparable to that of the human disease, resulting from striking neurogenic defects that include proliferative and survival defects in neuronal progenitors. *Cdk5rap2^an/an^* neuronal precursors exit the cell cycle prematurely and many undergo apoptosis. These defects are associated with impaired mitotic progression coupled with abnormal mitotic spindle pole number and mitotic orientation. Our findings suggest that the reduction in brain size observed in humans with mutations in *CDK5RAP2* is associated with impaired centrosomal function and with changes in mitotic spindle orientation during progenitor proliferation.

KEY WORDS: *CDK5RAP2*, Centrosome, Neurogenesis, Mouse

INTRODUCTION

The cerebral cortex that provides humans with our unique cognitive abilities consists of six morphologically and functionally distinct neuronal layers (Rakic, 2009). All cortical neurons are produced from a neuroepithelium lining the ventricular cavity of the developing brain (Noctor et al., 2001). During neurogenesis, postmitotic neurons differentiate and migrate away from the ventricular zone (VZ) towards their final destination in the cerebral cortex (Rakic, 2009). Earlier born neurons localize to deeper layers of the cortex, whereas later born neurons populate progressively more superficial layers (Angevine and Sidman, 1961; Rakic, 1974). Hence, proper development of the cerebral cortex requires the coordination of cell proliferation, fate determination and migration. Defects in these processes can cause neurodevelopmental disorders such as microcephaly, a disease associated with mental retardation (Mochida, 2008). Primary microcephaly is defined as decreased head circumference and a disproportionately reduced cerebral cortex, but no other major developmental malformations (Woods et al., 2005).

The centrosome plays key roles in neuronal progenitor proliferation and fate determination, as well as neuronal differentiation and migration (Higginbotham and Gleeson, 2007). Recent work suggests that asymmetric inheritance of daughter and mother centrosomes regulates cell fate determination in cortical progenitors (Wang et al., 2009). Moreover, mutations in several genes that encode centrosomal proteins cause human primary microcephaly (Woods et al., 2005). Among them is *CDK5RAP2* (cyclin-dependent kinase 5 related activator protein 2 or CDK5 regulatory subunit-associated protein 2) (Bond et al., 2005), which was originally identified in mammals by its interaction with p35[Nck5a] (p35; Cdk5r1), an activator of the neuronal cyclin-dependent kinase 5 (CDK5) (Ching et al., 2000). *CDK5RAP2* encodes a 1893 amino acid, 215 kDa centrosomal protein. In somatic cells, CDK5RAP2 promotes centrosomal cohesion (Graser et al., 2007) and recruits the γ-tubulin ring complex (γ-TuRC) – the microtubule nucleator – to the centrosome (Fong et al., 2008). However, the role of CDK5RAP2 in neuronal development remains poorly understood.

Hertwig's anemia (*an*) arose in the progeny of a heavily irradiated male mouse (Hertwig, 1942). Homozygous mutant animals have a macrocytic, hypoproliferative anemia and leukopenia attributable to intrinsic defects that are progressively more severe in the more mature hematopoietic progenitors (Barker and Bernstein, 1983; Barker et al., 2005; Eppig and Barker, 1989). Male animals are infertile due to severe deficiencies in germ cells, whereas female animals have less severe defects in oocytes, but cannot deliver pups (Russell et al., 1985). There is a high level of spontaneous aneuploidy in primary cultures of hematopoietic fetal liver, bone marrow and kidney epithelial cells derived from mutant animals (Eppig and Barker, 1984). Both the severity of the hematological disease and a coexisting predisposition to hematopoietic tumors are highly dependent upon the genetic background of the animal (Barker et al., 2005). Here, we show by

[1]Division of Genetics and the Manton Center for Orphan Disease Research, Children's Hospital Boston, Howard Hughes Medical Institute, Beth Israel-Deaconess Medical Center, and Departments of Pediatrics and Neurology, Harvard Medical School, 3 Blackfan Circle, Boston, MA 02115, USA. [2]Department of Pathology, Children's Hospital Boston and Harvard Medical School, 300 Longwood Avenue, Boston, MA 02115, USA. [3]Division of Hematology/Oncology, Children's Hospital Boston and Dana Farber Cancer Institute, Harvard Medical School, 1 Blackfan Circle, Boston, MA 02115, USA. [4]Brigham And Women's Hospital, 45 Francis Street, Boston, MA 02115, USA. [5]The Jackson Laboratory, 300 Main St, Bar Harbor, ME 04609, USA.

*Present address: Mount Sinai Medical School, Graduate Program in Biological Sciences, New York, NY 10029, USA
†Authors for correspondence (mark.fleming@childrens.harvard.edu; christopher.walsh@childrens.harvard.edu)

positional cloning that *an* is due to a mutation in *Cdk5rap2*, and that *an* mutants show additional severe neurological defects that were not previously recognized.

Mutations in human *CDK5RAP2* cause severely reduced brain size with relatively well-preserved cortical patterning (Bond et al., 2005), but without anemia or tumor predisposition, the hallmarks of *an*. Although CDK5RAP2 is one of several centrosomal proteins implicated in human microcephaly (Bond et al., 2002; Bond et al., 2005), we present the first analysis of any of these centrosomal proteins in mutant mice. Our analysis reveals important roles for Cdk5rap2 in mitotic progression and mitotic spindle orientation. Our data also suggest that Cdk5rap2 is essential for cortical progenitor proliferation and survival. These results illustrate the fundamental role of centrosome function in disease mechanisms associated with human primary microcephaly.

MATERIALS AND METHODS

Mouse strains and genetic mapping
We maintained the *Hertwig's anemia* (*an*) mutation on the WB/ReJ (WB) and C57BL/6J (B6) inbred backgrounds, as homozygous mutant mice are poorly viable, particularly on the C57BL/6J background. WB.Cg *an/+* × B6.Cg *an/+* F[1] (WBB6F1) animals are nearly fully viable and were used for studies in adults. To identify the gene underlying the *an* phenotype, we performed an intersubspecific intercross between B6.Cg *an/+* and the +/+ *Mus musculus castaneus* (CAST/Ei) inbred strain to generate second filial generation (F[2]) intercross animals segregating the *an* allele. F[2] animals were phenotyped by complete blood count at 3 weeks of age. We reconfirmed linkage to the *brown* locus on chromosome 4 in 46 consecutive F[2] animals at 3 weeks of age, and further delineated the genetic interval by genotyping an additional 734 F[2] animals and correlating the phenotype with crossover events within the originally defined locus. Genotyping and breeding of additional novel crossover events in the B6.Cg *an/+* colony further narrowed the critical region.

Genotyping
Subsequent to mutation identification, animals were genotyped using standard PCR reactions specific for the wild-type (1040 bp, primers 5′-TCACTGAGCTGAAGAAGGAGAA-3′ and 5′-GCAATCACTAAAAT-GTCCGATT-3′) and mutant (507 bp, primers 5′-GCAATCACTAAAAT-GTCCGATT-3′ and 5′-TGTCTTTCTGCCCTGACAGT-3′) alleles.

Northern blot analysis
Total RNA from *Cdkd5rap2an/an* and *Cdk5rap2+/+* tissue was extracted and purified as described (Baelde et al., 2001). A ^{32}P-labeled *Cdk5rap2* probe (500 bp) was generated by PCR amplification of exon 24 from mouse genomic DNA (129S6.Tac) with primers 5′-GCCTTATTACCAGCATG-CAA-3′ and 5′-TCACCGAAAAGTTCCAAGTTC-3′. A commercial mouse multi-tissue northern blot (Origene) and the *Cdk5rap2an/an* and *Cdk5rap2+/+* blot were run, transferred, hybridized and processed as previously described (Lee et al., 2007).

Immunoblotting
Cdk5rap2+/+ and *Cdk5rap2an/an* tissues were homogenized and protein extracted in RIPA buffer (50 mM Tris-HCl pH 7.2, 150 mM NaCl, 0.5% sodium deoxycholate, 0.1% SDS, 1% Nonidet P40) with Complete Protease Inhibitors (Roche). Protein (30 μg per sample) was loaded onto a 7% Novex Tris-acetate gel (Invitrogen) and run according to the manufacturer's instructions. Gels were transferred to nitrocellulose membranes using a semi-dry transfer system (Hoeffer) and analyzed with rabbit anti-Cdk5rap2 antibody at 1:1500 (Bethyl Laboratories).

Histology and immunostaining
Embryonic and postnatal day 0 (P0) brains were dissected in ice-cold 1×PBS, fixed in 4% paraformaldehyde by immersion or cardiac perfusion, embedded in paraffin and sectioned at 5 μm. Immunohistochemistry was performed as previously described (Feng and Walsh, 2004). Animals were handled according to protocols approved by the IACUC of the Beth Israel Deaconess Medical Center and the Children's Hospital Boston.

Antibodies
The following antisera were used at the specified dilutions: rabbit anti-Cdk5rap2 (1:1000) (Bethyl laboratories, BL2320); rabbit anti-Ki67 (1:500) (Vector Labs, VP-RM04); rabbit anti-Dcx (1:500) (Covance); goat anti-Cux1 (1:10) (Santa Cruz, SC6327); rat anti-Ctip2 (1:500) (Abcam, ab18465); mouse anti-aurora kinase A (1:200) (Abcam, ab13824); rabbit anti-Tbr2 (1:300) (Abcam, ab23345); rabbit anti-phospho-histone H3 (1:500) (Upstate, 07-492); rabbit anti-Sox2 (1:200) (Novus-Biologicals, NB110-372335C); rat anti-BrdU (1:300) (abdSerotec, MCA2060); rabbit anti-Tbr1 (1:500) (gift from R. Hevner, University of Washington, Seattle, WA, USA); goat anti-Brn1 (1:200) (Santa Cruz, SC-6028); mouse anti-aurora kinase B (1:200) (BD biosciences, 611083); rabbit anti-Par3 (1:300) (Upstate, 07-330); and rabbit anti-activated cleaved caspase 3 (1:50) (Cell Signaling, 9661). Secondary detection reagents (1:500) included Alexa Fluor 488-, 594- or 546-conjugated anti-rabbit, mouse or goat IgG (Invitrogen); Cy5-conjugated anti-rabbit, mouse or goat IgG, Cy3-conjugated or unconjugated Fab fragments of anti-rabbit IgG (Jackson ImmunoLaboratories); and Cy3-conjugated Streptavidin reagent.

Analysis of cells in S phase and of cell cycle exit
For analysis of S-phase cells, E10.5 and E14.5 pregnant females were injected intra-peritoneally with 70 μg BrdU/g body weight and sacrificed 30 minutes after injection. The percentage of cells in S phase was calculated by counting cells stained with BrdU as a function of total nuclei. For analysis of cell cycle exit, E14.5 pregnant females were injected with BrdU as above, sacrificed 24 hours after injection, and analyzed as previously described (Chenn and Walsh, 2002).

Image acquisition and data analysis
Images were acquired and analyzed as previously described (Sepp et al., 2008). For spindle orientation analysis, images were acquired as 5 μm z-stacks using a Zeiss confocal microscope and angles were measured in three-dimensional (3D) reconstructed projections using ImageJ (NIH). At least three coronal brain serial sections from at least three different animals were analyzed per genotype per experiment. Unless otherwise noted, brain sections were chosen at the mid-anterior level of the brain, and micrographs were taken of the dorsal and dorsal-lateral cortex region. Cell counts were performed as a percentage of total nuclei per high-magnification field per coronal section. *P*-values were calculated with an ANOVA single-factor test.

RESULTS

Hertwig's anemia is due to a mutation in *Cdk5rap2*
We mapped *Hertwig's anemia* (*an*) to a 290 kb genomic interval between 68.91 and 69.94 Mb (genomic assembly NCBI m35, Dec 2005; www.ensembl.org/mus_musculus) on mouse chromosome 4, which includes the 5′ end of *Cdk5rap2* and the multiple epidermal growth factor-like domains 9 (*Megf9*) gene. Sequencing of the entire coding regions of *Megf9* and *Cdk5rap2* revealed no exonic or splice junction mutations. However, RT-PCR of *Cdk5rap2* from WBB6F1 *an/an* animals demonstrated an in-frame 111 bp deletion resulting from loss of exon 4 from the mRNA (see Fig. S1A in the supplementary material). This change predicts a 37 amino acid deletion of Cdk5rap2, but as the mutant mRNA maintains the reading frame a shortened protein product could be formed (see Fig. S1B in the supplementary material). Northern analysis demonstrated that exon 4 was uniformly omitted from the mutant mRNA (Fig. 1A). Amplification of genomic DNA indicated that the basis of this exon skipping was an inversion of exon 4 (Fig. 1B). Furthermore, B6.Cg *an/+* females bred to male animals chimeric for a *Cdk5rap2* gene-trap allele yielded F[1] compound heterozygous animals with leukopenia and macrocytic anemia, similar to the *an* mutants (see Table S1 in the supplementary material), confirming *Cdk5rap2* as the *Hertwig's anemia* gene and allowing the designation of the mutation as *Cdk5rap2an*.
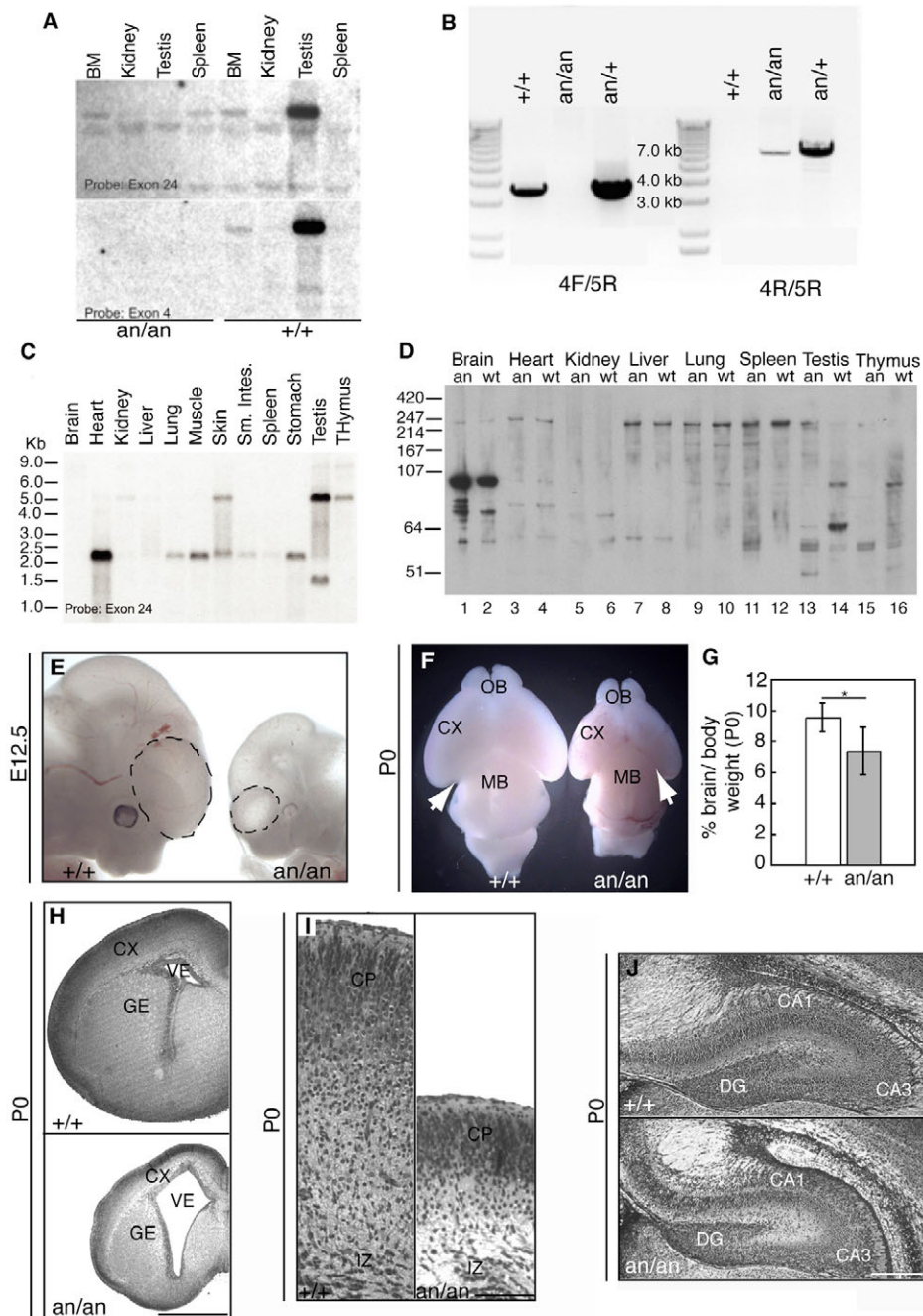
Fig. 1. *Hertwig's anemia (an)* is due to an inversion of exon 4 of *Cdk5rap2*, resulting in exon 4 skipping and abnormal cortical development. (**A**) Exon 4 is skipped in *an/an* homozygotes. *Cdk5rap2* expression is detected in both +/+ and *an/an* mice using an exon 24 probe (upper panel). However, reprobing the same blot with an exon 4 probe yields no signal in *an/an* animals (lower panel). (**B**) PCR of genomic DNA from +/+, *an/+* and *an/an* WBB6F1 confirmed the presence of an inversion surrounding exon 4. (**C**) Northern blot of adult mouse tissues demonstrating a 2.3 kb transcript expressed in most tissues, a 5.8 kb transcript expressed in several tissues and particularly strongly in testis, and a 1.4 kb transcript expressed only in testis. (**D**) Western analysis of Cdk5rap2 protein in +/+ and *an/an* adults. Most tissues have a large (~230 kDa) isoform, whereas the testis, thymus and brain also contain a smaller (~105 kDa) isoform. A testis-specific protein isoform (~70 kDa) is also observed. (**E**) B6.Cg *an/an* embryos have reduced brain and body sizes already at E12.5, as compared with controls. Dashed lines highlight cortical vesicles. (**F**) Transmitted light micrograph of P0 B6.Cg *Cdk5rap2*^{+/+} and *Cdk5rap2*[an/an] brains. Mutant brains are smaller with a disproportionately reduced cortex (CX) and smaller olfactory bulbs (OB). Arrows indicate that more of the midbrain (MB) area is exposed in *Cdk5rap2*[an/an] than in the control. (**G**) Analysis of the brain-to-body weight ratio in the B6.Cg background, showing that the mean brain-to-body weight ratio at P0 is decreased in *Cdk5rap2*[an/an] animals. Error bars indicate s.d. *, $P=7\times10^{-5}$. (**H**) Histological analysis of P0 brains from B6.Cg animals. Coronal sections (5 μm) stained with Cresyl Violet show a thinner cortex, reduced ganglionic eminence (GE) and enlarged ventricle (VE) in the mutants. (**I**) At P0, the cortex of *Cdk5rap2*[an/an] animals is smaller but shows a laminar organization that is similar to that of control littermates. A high-magnification micrograph shows the cortical plate (CP) and intermediate zone (IZ) in control (left) and mutant (right) animals. (**J**) At P0, the hippocampus is smaller in *Cdk5rap2*[an/an] (bottom) than in controls (top). DG, dentate gyrus; CA1 and CA3, cornus ammonis 1 and 3. Scale bars: 200 μm in H; 100 μm in I,J.

Expression analysis of *Cdk5rap2* and *Cdk5rap2ⁿ*

Cdk5rap2ᵃⁿ/ᵃⁿ animals had defects in multiple organs, including brain, thymus and testis. Using a probe to exon 24, we found that the predominant *Cdk5rap2* transcript differs from tissue to tissue, with a 5.8 kb major transcript in testis and thymus, and a 2.3 kb transcript most abundant in heart and most other tissues (Fig. 1C). A unique 1.4 kb transcript was also present in testis. Although the mRNA was undetectable in adult brain using a probe to exon 24, the GENSAT in situ hybridization reference database (www.ncbi.nlm.nih.gov/projects/gensat/) and published work (Bond et al., 2005) show that *Cdk5rap2* is highly expressed in embryonic neural progenitors.

Immunoblotting of Cdk5rap2 protein in the mutant indicated that deletion of exon 4 does not substantially destabilize the protein. In most tissues, a large (~230 kDa) species was seen to predominate. A smaller isoform (~105 kDa) was present in testis and thymus and predominated in adult brain, but was barely detectable in fetal brain or other tissues (Fig. 1D and data not shown). This suggests that the 230 kDa isoform disrupted in *Cdk5rap2ᵃⁿ/ᵃⁿ* animals is the predominant functional species in fetal brain. The major protein isoforms might correspond to the two largest of the three mRNAs. Furthermore, as in the northern analysis (Fig. 1C), there was an additional testis-specific protein isoform (~70 kDa). All of these proteins isoforms are too large to permit the resolution of a shortened *an* mutant protein by western analysis.

Cdk5rap2 is essential for normal brain development

The identification of *Cdk5rap2* as the *an* gene prompted us to examine the brain of *an* mutants, which had not previously been evaluated. WBB6F1 hybrid *Cdk5rap2ᵃⁿ/ᵃⁿ* adult animals showed moderate cortical hypoplasia visualized by shortening of the forebrain, which did not extend fully over the superior colliculus of the midbrain, as it does in normal animals (see Fig. S1C in the supplementary material). However, inbred B6.Cg *Cdk5rap2ᵃⁿ/ᵃⁿ* animals showed a dramatic reduction in brain size and rarely survived beyond 1 week of age. They were runted, with disproportionately smaller brains both prenatally and at birth (Fig. 1E,F). The mutants exhibited a significant decrease in the ratio of brain to body weight as compared with controls (7.5 ± 1.5 versus 9.5 ± 0.9 mg/g, $P<1\times10^{-4}$) (Fig. 1G). The brain phenotype had a variable expressivity, being more severe in some individuals than others (Fig. 1E,F), including variably increased ventricular size and variably decreased cortical thickness (Fig. 1H,I). Other brain structures, including the hippocampus, were also considerably smaller than normal (Fig. 1J). Together, these data demonstrate that Cdk5rap2 is essential for normal brain development.

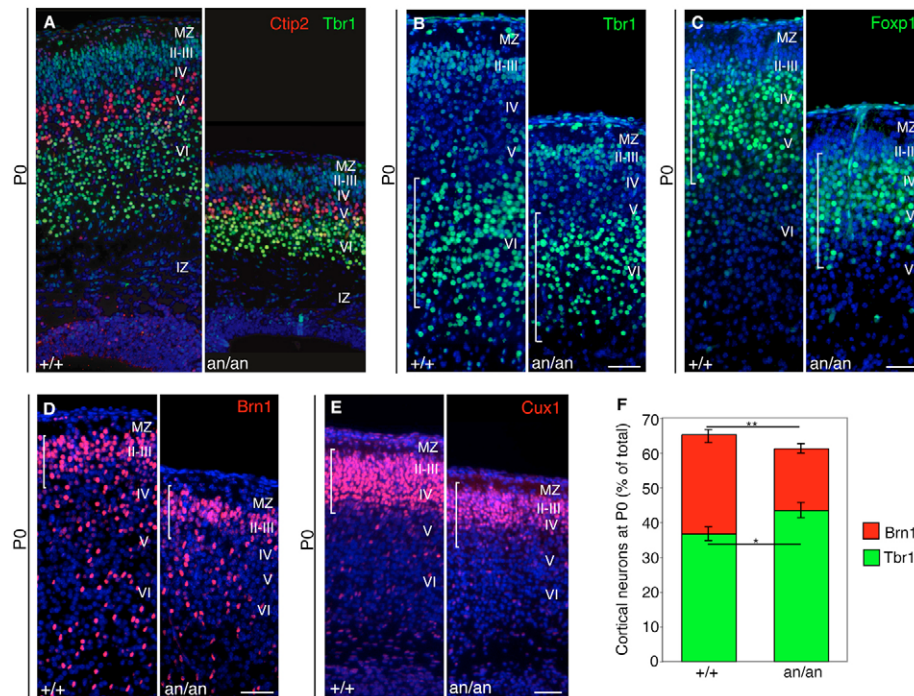## Cdk5rap2ᵃⁿ/ᵃⁿ mice show reduced superficial cortical layers

The cortical neuronal layers are formed in an 'inside-out' fashion, whereby the deepest layers form first and the most superficial layers form last (Rakic, 2009). In newborn (P0) *Cdk5rap2ᵃⁿ/ᵃⁿ* animals, immunostaining for Tbr1 and Ctip2 (Bcl11b – Mouse Genome Informatics) (layers V-VI) (Hevner et al., 2001; Leid et al., 2004), Foxp1 (layers III-V) (Ferland et al., 2003), Brn1 (Pou3f3) and Cux1 (layers II-IV) (McEvilly et al., 2002; Nieto et al., 2004) showed profound defects in neurogenesis but relatively preserved cortical layering (Fig. 2A-E), suggesting that neuronal migration was generally normal. However, *Cdk5rap2ᵃⁿ/ᵃⁿ* mice showed consistent thinning of the cerebral cortex (Fig. 2A and see Fig. S2A,B in the supplementary material), accompanied by preferential reduction of the superficial, later-born neuronal layers (Fig. 2D-F), as demonstrated by a significant decrease in Brn1-positive cells compared with controls ($17.8\pm1.4\%$ versus $28.6\pm2.43\%$, $P<1\times10^{-9}$). The preferential decrease of superficial neurons in mutant animals was confirmed by Cux1 immunostaining (Fig. 2E). The dramatic decrease in superficial layers resulted in fewer total cells and was associated with correspondingly increased early-born, Tbr1-positive cells in mutants as compared with controls ($43.4\pm2.2\%$ versus $36.7\pm1.9\%$, $P<0.001$) (Fig. 2B,C,F). Thus, *Cdk5rap2ᵃⁿ/ᵃⁿ* animals have fewer total neurons and the last-born superficial neurons are particularly reduced.

Cdk5rap2ᵃⁿ/ᵃⁿ mice have defects in neurogenesis during development

Our observations in newborn animals prompted us to investigate the effect of the *Cdk5rap2ᵃⁿ/ᵃⁿ* mutation during embryonic development. We found a significant decrease in overall cortical thickness at E13.5 (Fig. 3A,B), indicating a defect at early stages of neurogenesis. Immunostaining for Dcx, which marks immature neurons (Gleeson et al., 1999), showed that E15.5 *Cdk5rap2ᵃⁿ/ᵃⁿ* embryos had a thinner neuronal layer than controls, expressed as the ratio of the thickness of Dcx-immunolabeled neuronal layers over total cortical thickness ($43.9\pm1.6\%$ versus $58.3\pm2.4\%$, $P<0.001$) (Fig. 3C,D). The decrease in cortical neurons was associated with a reduction in the precursor population, as revealed by immunoreactivity for Ki67 (Mki67), a marker of dividing cells, which was diminished in E16.5 *Cdk5rap2ᵃⁿ/ᵃⁿ* embryos compared with controls (141.1 ± 9 versus 185 ± 5, $P<0.01$) (Fig. 3E,F). In addition, short pulses of BrdU at E10.5 (when the developing cortex is primarily composed of neuronal progenitors) and at E14.5 (when most of the deeper layers have already formed), showed that *Cdk5rap2ᵃⁿ/ᵃⁿ* embryos have a progressive decrease in the density of S-phase cells (see Fig. S3A-C in the supplementary material), suggesting that progenitor cells decrease as development proceeds.

Neuronal progenitors form two groups that undergo mitosis either at the apical surface of the ventricle or on the basal side away from the VZ (Gotz and Huttner, 2005), and both progenitor types were affected in *Cdk5rap2ᵃⁿ/ᵃⁿ* mutants. Apical progenitors give rise to deep layer neurons and basal progenitors, whereas basal progenitors primarily produce superficial layer neurons (Pontious et al., 2008). Radial glial cells, a subset of apical progenitors, produce most CNS neurons and provide a scaffold for newly formed neurons to migrate (Misson et al., 1988). We immunostained E15.5 *Cdk5rap2ᵃⁿ/ᵃⁿ* mice for Glast (Slc1a3 – Mouse Genome Informatics), a radial glial marker (Shibata et al., 1997), and found no apparent changes in their morphology (data not shown), although the decreased Ki67 and Sox2 staining (Fig. 3E-J) suggested that their number was reduced. In addition, E14.5 and E16.5 *Cdk5rap2ᵃⁿ/ᵃⁿ* embryos showed a marked loss of basal progenitors upon immunostaining for the basal progenitor marker Tbr2 (Eomes – Mouse Genome Informatics) (Englund et al., 2005) and for Sox2, a marker for apical progenitors and a subset of basal progenitors (Bani-Yaghoub et al., 2006) (Fig. 3G-I). The ratio of Tbr2-positive cells to total progenitors was decreased in mutants at both E14.5 ($28.9\pm1.8\%$ versus $40.8\pm2.2\%$, $P<5\times10^{-4}$) and E16.5 ($34.5\pm1.2\%$ versus $43.8\pm1.1\%$, $P<1\times10^{-5}$) (Fig. 3I), demonstrating that the decrease in superficial layer neurons correlates with a reduction in basal progenitors. Interestingly, at mid-neurogenesis, a fraction of these Tbr2-positive cells normally localizes to the VZ, whereas in mutant animals fewer Tbr2-positive cells were located within the VZ. Whereas E15.5 control embryos had roughly an

Fig. 2. Cdk5rap2$^{an/an}$ mice show reduced neuronal number and thinner superficial layers but preserved cortical layer organization. (**A**) Cdk5Rap2 mutant mice show preserved cortical layer organization, although each layer is far thinner than normal. P0 wild-type (+/+) and mutant (an/an) littermates are shown. Coronal sections stained with Tbr1 antisera, which labels deep layer VI neurons (green), and with Ctip2 antisera, which labels layer V neurons (red), show the preservation of cortical layer organization in the mutant. The marginal zone (MZ) and IZ are also shown. (**B,C**) Deeper cortical layer markers show the overall reduction in cortical thickness in the an/an mutant. (B) Tbr1, layer VI; (C) Foxp1, layers III-V. (**D,E**) Superficial cortical layers are reduced in the Cdk5Rap2$^{an/an}$ brain. P0 wild-type (+/+) and mutant (an/an) littermate coronal sections stained with antisera against (D) Brn1 (layers II-III) and (E) Cux1 (layers II-IV). In B-E the brackets correspond to wild type and highlight the differences between mutant and control animals. (**F**) The density of superficial and deeper neuronal layers. The density of layers II-III was calculated as the ratio of Brn1-positive cells to total CP nuclei counted per section (the mean percentage is shown). The Brn1 density (red bars) in wild-type (n=6 animals, 486 cells counted/section) and mutant (n=7 animals, 417 cells counted/section) animals is significantly different; **, $P=7.4 \times 10^{-10}$. The corresponding increase in the density of deep neuronal layer VI is shown. The percentage of Tbr1-positive cells (green bars) among total CP nuclei is moderately increased in the mutant (n=5 animals, 431 cells counted/section) as compared with control littermates (n=6 animals, 544 cells counted/section); *, $P=1.3 \times 10^{-4}$. Sections were counterstained with Hoechst 33342 (blue) to label nuclei. Error bars indicate s.e.m. Scale bars: 50 μm.

equal distribution of Tbr2-positive cells in the VZ (93.2±17.8) and subventricular zone (SVZ) (101.7±11.3), Cdk5rap2$^{an/an}$ embryos had 59.8% fewer Tbr2-positive cells within the VZ (38.4±5.9) compared with the SVZ (64.2±2.6) (Fig. 3J). This profound reduction of basal progenitors at later stages in neurogenesis might reflect a more generalized loss of all progenitors over the course of neurogenesis, although a more specific defect in basal progenitors cannot be ruled out.

## Mitotic abnormalities in Cdk5rap2$^{an/an}$ mice

Since Cdk5rap2 is a centrosomal protein, we hypothesized that the neuronal progenitor deficiency in Cdk5rap2$^{an/an}$ animals reflects underlying mitotic defects. Using the mitotic (M)-phase marker phospho-histone H3, we analyzed E12.5 (see Fig. S4 in the supplementary material), E14.5 and E16.5 embryos (Fig. 4A,B). We found 1.8-fold more M-phase cells in mutants compared with controls at E16.5 (61.75±6.24 versus 35.26±4.8, $P<1\times10^{-7}$). This increase in mitotic cells reflected increases at the luminal VZ (45.95±5.57 versus 28.57±4.23, $P<1\times10^{-5}$) and outside the VZ (13.07±1.81 versus 5.78±1.27, $P<1\times10^{-7}$) (Fig. 4C). Since the overall progenitor number decreases, this surprising increase in M-phase cells suggests that Cdk5rap2 deficiency leads to a delay in

mitotic progression. To determine the cause of this delay, we examined aurora kinase A immunoreactivity (Katayama et al., 2003) in neuronal precursors. Aurora kinase A labels the mitotic spindle poles as two distinct dots at the focused ends of a bipolar spindle structure. Cdk5rap2$^{an/an}$ embryos showed a 2.8-fold increase in pro-metaphase and metaphase precursor cells with mono-, tri- and other aneupolar spindle poles labeled with aurora kinase A, as compared with controls (12.95±3.26% versus 4.62±1.69%, $P<1\times10^{-5}$) (Fig. 4D,E). These abnormal spindles confirm previous data indicating that atypical meioses are readily apparent in Cdk5rap2$^{an/an}$ embryonic germ cells and suggests a mechanism for the predisposition to chromosomal aneuploidy seen in Cdk5rap2$^{an/an}$ primary cells (Eppig and Barker, 1984).

Cdk5rap2$^{an/an}$ cortical progenitors have defective mitotic spindle orientation

During neurogenesis, the orientation of the mitotic division plane relative to the ventricular surface (VS) has been proposed to influence cell fate determination (Zhong and Chia, 2008). The disruption of proteins that regulate mitotic spindle orientation at the VZ correlates with premature and excessive generation of neurons and early depletion of cortical progenitors (Feng and Walsh, 2004;
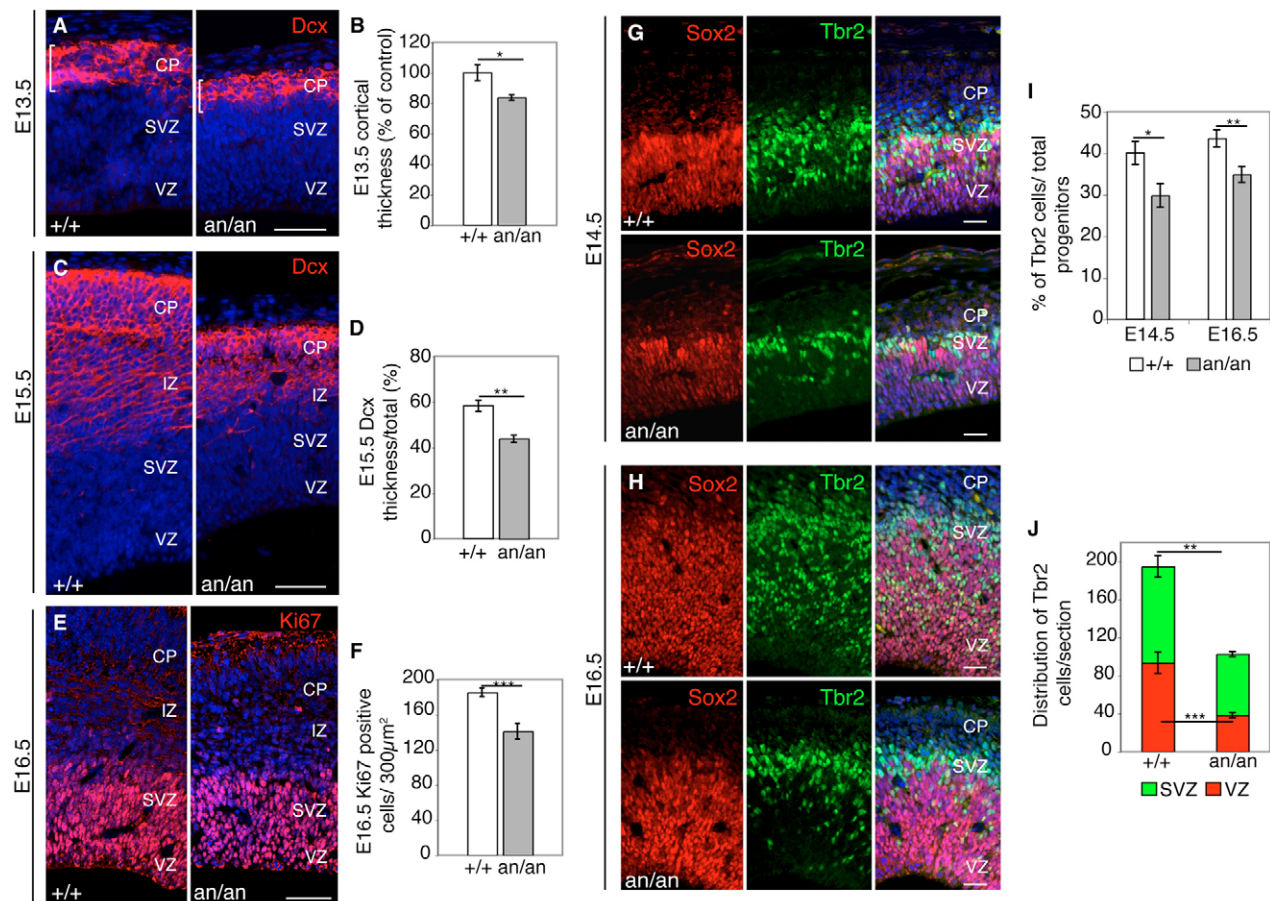
Fig. 3. Neurons and neuronal progenitors are reduced in *Cdk5rap2^an/an* mice. (**A**) E13.5 coronal sections immunostained for Dcx (a marker for immature neurons) in wild-type (+/+) and mutant (*an/an*) littermate pairs. (**B**) Overall cortical thickness is reduced at E13.5 in *Cdk5rap2^an/an* animals (*n*=5) compared with controls (*n*=3). The mean is shown as a percentage of the control mean (+/+, 100±5.2%; *an/an*, 83.9±1.8%); *, *P*=0.001. (**C**) E15.5 coronal sections show a significantly reduced CP in mutants. (**D**) CP thickness at E15.5 in mutants and controls (*n*=4) shown as the ratio of Dcx-positive cortical thickness over total cortical thickness. **, *P*=6.3×10⁻⁴. (**E**) Total proliferating cells are reduced in the mutants (*n*=7) compared with controls (*n*=4). Coronal sections of E16.5 littermates were analyzed by Ki67 immunostaining. (**F**) Quantitation of proliferating cells, showing the total number of Ki67-positive cells counted per 300 μm². ***, *P*=0.002. (**G,H**) Coronal sections of E14.5 and E16.5 littermates were analyzed using Tbr2 (green), a marker for basal progenitors, and Sox2 (red), a marker for neuronal progenitors. (G) E14.5 embryos show some Tbr2-labeled cells in the VZ, SVZ and CP. (H) At E16.5, the reduction in Tbr2-positive cells is also evident across the VZ and SVZ in *Cdk5rap2^an/an* embryos. (**I**) At E14.5, *Cdk5rap2^an/an* embryos (*n*=5, 214 cells counted/section) had 11.9% fewer Tbr2-positive cells than *Cdk5rap2^+/+* (*n*=5, 366 cells counted/section); *, *P*=2×10⁻⁴. At E16.5, *Cdk5rap2^an/an* embryos (*n*=5, 420 cells counted/section) had 9.3% fewer Tbr2-positive cells than *Cdk5rap2^+/+* (*n*=5, 630 cells counted/section); **, *P*=1.3×10⁻⁶. (**J**) The distribution of Tbr2-positive cells changes in the *Cdk5rap2^an/an* animals. The mean number of Tbr2-positive cells is shown for the VZ and the SVZ. Control embryos had 2.4-fold more Tbr2-positive cells in the VZ and 1.5-fold more in the SVZ than the mutants. **, *P*=0.01; ***, *P*=0.003. Error bars indicate s.e.m. (B,D,F,I) or s.d. (J). Scale bars: 50 μm in A,C,E; 200 μm in G,H.

Fish et al., 2006; Sanada and Tsai, 2005), although the relevance of this mechanism to human microcephaly has been uncertain. To investigate mitotic orientation during neurogenesis in *Cdk5rap2^an/an* mice we focused on anaphase and telophase spindles, as metaphase spindles undergo dynamic rotations (Haydar et al., 2003). We defined cleavage plane orientations in relation to the VS as horizontal (0-30°, i.e. mitotic spindle aligned parallel to the VS), oblique (30-60°) or vertical (60-90°, i.e. mitotic spindle aligned along the apical-basal axis of the VS) (Chenn and McConnell, 1995). During cortical development, most cleavage planes are oriented perpendicular to the VS, producing side-by-side daughter cells (Zhong and Chia, 2008). By co-immunostaining for Par3 (Pard3 – Mouse Genome Informatics) to label the VS (Bultje et al., 2009) and aurora kinase B to label the central spindle (anaphase) and the midbody (telophase) (Vader and Lens, 2008),

we found increased horizontal cleavage planes in *Cdk5rap2^an/an* mice compared with controls at E14.5 (15.6±3.2% versus 7.7±4.0%, *P*<0.05) (see Fig. S5 in the supplementary material). E16.5 *Cdk5rap2^an/an* embryos had increased horizontal cleavage planes (21.2±4.5% versus 10.0±2.6%, *P*<0.01) and reduced vertical cleavage planes (37.2±7.1% versus 56.1±5.8 %, *P*<0.01) (Fig. 4F). Thus, Cdk5rap2 is important for mitotic spindle orientation in cortical progenitors.

Cdk5rap2^an/an neuronal progenitors show premature cell cycle exit and increased cell death

Mutation of *Nde1*, which encodes another spindle pole protein, causes premature cell cycle exit of neuronal progenitors, depleting the progenitor pool prematurely and reducing brain size (Feng and Walsh, 2004). To investigate whether similar processes cause
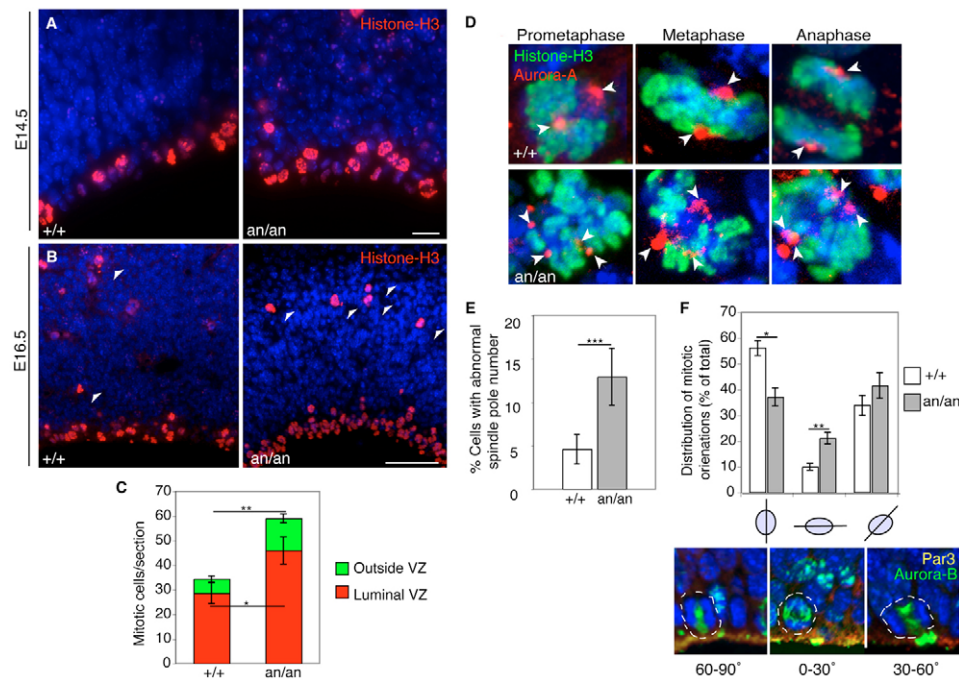
Fig. 4. *Cdk5rap2^{an/an}* neuronal progenitors exhibit mitotic defects and changes in mitotic spindle orientation. (**A**,**B**) *Cdk5rap2* mutants have increased numbers of phospho-histone H3-labeled cells. Fluorescent micrographs of *Cdk5rap2^{+/+}* and *Cdk5rap2^{an/an}* coronal sections at (A) E14.5 and (B) E16.5. Phospho-histone H3 (red) immunostaining shows cells in M phase lining the VZ, and away from the VZ (arrowheads). Nuclei are stained with Hoechst (blue). (**C**) Analysis of mitotic index in E16.5 embryos. M-phase cells counted along the luminal VZ from the medial-dorsal to the dorsal-lateral junction. Dorsal mitotic cells away from the VZ were also measured. The mean total mitotic cells per coronal section and their localization at the luminal VZ, or away from the VZ, are shown. At E16.5, *Cdk5rap2^{an/an}* mice ($n=5$, average of 330 mitotic cells counted/animal) had 1.8-fold more M-phase cells than controls ($n=5$, average of 128 mitotic cells counted/animal; $P=1.12 \times 10^{-8}$. M-phase cells increased at the luminal VZ (*, $P=5.64 \times 10^{-6}$) and outside of the VZ (**, $P=2.22 \times 10^{-8}$). (**D**) *Cdk5rap2^{an/an}* animals have abnormal numbers of spindle poles. Aurora kinase A labels spindle poles (red), whereas phospho-histone H3 labels M-phase cells (green). Arrowheads indicate aurora kinase A-labeled spindle poles. Representative confocal images of *Cdk5rap2^{+/+}* precursor cells (top) in prometaphase (left), metaphase (center) and anaphase (right) with bipolar spindles, and *Cdk5rap2^{an/an}* precursor cells (bottom) in prometaphase with a tetrapolar spindle (left), in metaphase with a tripolar spindle (center), and in anaphase with a tetrapolar spindle (right). (**E**) *Cdk5rap2^{an/an}* animals show a 2.8-fold increase in the percentage of abnormal mitotic figures per total number of M-phase cells at the luminal VZ. ***, $P=3.26 \times 10^{-6}$. (**F**) Analysis of spindle orientation at E16.5. Bar chart shows the distribution of horizontal (0-30°), oblique (30-60°) and vertical (60-90°) cleavage planes. *Cdk5rap2^{an/an}* embryos have increased horizontal and decreased vertical cleavage planes ($n=4$, average of 88 cells counted/animal; **, $P=0.005$), compared with *Cdk5rap2^{+/+}* embryos ($n=4$, average of 89 cells counted/animal; *, $P=0.006$). Beneath are shown representative three-dimensional reconstructed confocal images of horizontal, oblique and vertical cleavage planes. Nuclei are stained with Hoechst (blue), the central spindle and midbody are stained for aurora kinase B (green), and the apical membrane is stained for Par3 (yellow). Error bars indicate s.d. Scale bars: 10 μm in A; 50 μm in B.

progenitor cell deficits in *Cdk5rap2^{an/an}* animals, we labeled progenitors with BrdU at E14.5 and examined the fraction remaining in the cell cycle at E15.5 by double immunostaining for BrdU and the proliferation marker Ki67 (Chenn and Walsh, 2002). The 'exit fraction' (Caviness et al., 2003), representing the ratio of BrdU-positive Ki67-negative cells over total BrdU-positive cells, was increased by 25% in mutants compared with controls ($P<1 \times 10^{-4}$) (Fig. 5A,B), and this may contribute to the premature decrease in progenitors seen in *Cdk5rap2^{an/an}* embryos.

Defects in spindle orientation also correlate with increased cell death during neuroepithelial stem cell divisions (Yingling et al., 2008). We analyzed cells undergoing apoptosis by immunostaining for activated cleaved caspase 3 (caspase 3). Prior to the onset of neurogenesis (E10.5) we found 4.5-fold more apoptotic cells in mutants compared with control littermates ($12.7\pm4.4\%$ versus $2.8\pm1.6\%$, $P<1 \times 10^{-5}$), suggesting that these increased dying cells represent apical progenitors, the predominant cell type at this stage. At E12.5 we found a 6.8-fold

increase in cell death in *Cdk5rap2^{an/an}* animals compared with controls ($16.3\pm3.1\%$ versus $2.4\pm1.5\%$, $P<1 \times 10^{-9}$) (Fig. 5C-E). To investigate whether a particular cell type was targeted for cell death, we first analyzed the distribution of apoptotic cells in apical (alongside the ventricle), basal (away from the ventricle) and cortical plate (CP) regions at E12.5 (Fig. 5F,G). *Cdk5rap2^{an/an}* animals had more dying cells than controls in both apical (12.3 ± 3.1 versus 1.6 ± 0.7, $P<1 \times 10^{-5}$) and basal (40.5 ± 10.9 versus 2.8 ± 1.1, $P<1 \times 10^{-5}$) regions, as well as in the CP (20.4 ± 1.0 versus 3.8 ± 2.4, $P<1 \times 10^{-5}$) (Fig. 5G). Double immunostaining for Tuj1 (Tubb3 – Mouse Genome Informatics) and caspase 3 showed increased neuronal cell death in the mutants (Fig. 5F,G). Similarly, immunoreactivity of Tbr2 and caspase 3 showed increased cell death of basal progenitors in *Cdk5rap2^{an/an}* animals compared with controls ($46.0\pm3.7\%$ versus $8.7\pm4.9\%$, $P<1 \times 10^{-9}$) (Fig. 5H,I). Together, these data suggest that both the precursor and neuronal populations are probably susceptible to cell death in the *Cdk5rap2* mutants.
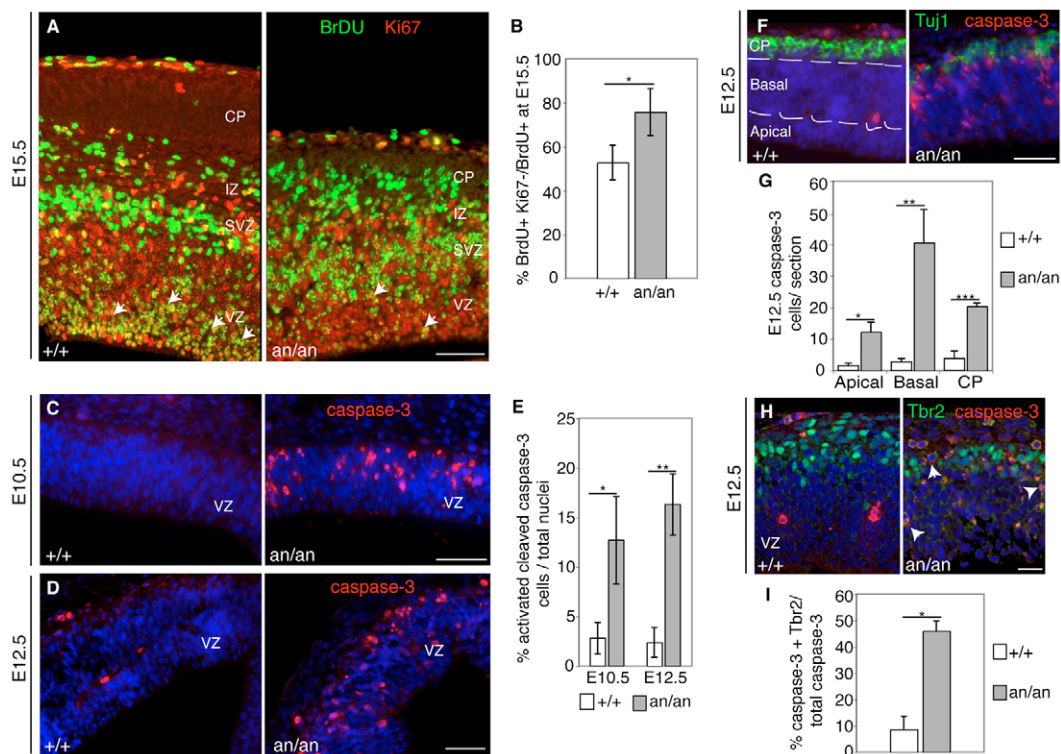
Fig. 5. Cdk5Rap2^{an/an} embryos exhibit increased cell death and premature cell cycle exit. (**A**) Increased cell cycle exit in Cdk5Rap2^{an/an} mice. An E14.5 pregnant female was injected with BrdU and sacrificed after 24 hours. BrdU-labeled progenitors (green) that remain in the cell cycle at E15.5 were identified by co-immunostaining for Ki67 (red). E15.5 Cdk5Rap2^{+/+} (n=5) and Cdk5Rap2^{an/an} (n=6) embryos were analyzed to determine the fraction of cells leaving the cell cycle by counting BrdU-positive Ki67-negative cells as compared with the total number of BrdU-positive cells. More cells labeled exclusively with BrdU are seen in the IZ and CP of Cdk5Rap2^{an/an}. Greater numbers of cycling cells labeled with both BrdU and Ki67 are found in the VZ of Cdk5Rap2^{+/+} (arrows). However, Cdk5Rap2^{an/an} had fewer cells that remained in the cell cycle (arrows). (**B**) Analysis of the 'exit fraction' in E15.5 littermates. The mean percentage of BrdU-positive Ki67-negative among total cells is shown for Cdk5Rap2^{+/+} (336 cells counted/animal) and Cdk5Rap2^{an/an} (420 cells counted/animal). *, $P=4.2\times10^{-5}$. (**C,D**) Cdk5Rap2^{an/an} animals show increased apoptosis. Coronal sections of (C) E10.5 and (D) E12.5 control and mutant embryos labeled with caspase 3 antibodies (red) and stained with Hoechst (blue) for nuclei. (**E**) The mean percentage of caspase 3-labeled cells in E10.5 and E12.5 embryos. Analysis of E10.5 littermates showed that Cdk5Rap2^{an/an} embryos (n=3 animals, 293 cells counted/section) had a 4.5-fold increase in the percentage of apoptotic cells as compared with controls (n=3 animals, 354 cells counted/section); *, $P=1.7\times10^{-6}$. Cdk5Rap2^{an/an} E12.5 embryos (n=4 animals, 419 cells counted/section) had 6.8-fold more cell death than controls (n=4 animals, 503 cells counted/section); **, $P=1.7\times10^{-13}$. (**F**) Cdk5Rap2^{an/an} E12.5 embryos show a higher index of apoptotic neuronal precursor and neuronal cells. Caspase 3-positive cells (red) are present in the apical, basal and CP regions. CP is shown by Tuj1 (green) immunostaining. (**G**) The average number of caspase 3-labeled cells in each region in E12.5 embryos. Cdk5Rap2^{an/an} embryos (n=3 animals, 73 dying cells counted/section) had 7.7-fold more dying cells in the apical region (*, $P=5.8\times10^{-6}$), 14.4-fold more apoptosis in the basal region (**, $P=2.9\times10^{-6}$), and 5.3-fold more cell death in the CP (***, $P=5.7\times10^{-6}$) than controls (n=3 animals, 8.2 dying cells counted/section). (**H**) Cdk5Rap2^{an/an} E12.5 embryos have a higher percentage of Tbr2 (green) and caspase 3 (red) double-positive cells (arrows) than controls. (**I**) The percentage of Tbr2 and caspase 3 double-labeled cells among the total caspase 3-positive cells in Cdk5Rap2^{an/an} (n=3 animals, 370 cells counted/section) and in controls (n=4 animals, 466 cells counted/section); *, $P=2.6\times10^{-10}$. Error bars indicate s.d. (B,E) or s.e.m. (G,I). Scale bars: 50 μm in A; 25 μm in C,D,F; 20 μm in H.

DISCUSSION

Here, we show that *Cdk5rap2* is mutated in the *Hertwig's anemia* mouse, and we demonstrate that Cdk5rap2 is essential for normal progenitor proliferation and survival in the cerebral cortex. *Cdk5rap2^{an/an}* animals have smaller cerebral cortices that result from an overall reduction of the neuronal layers caused by a decrease in progenitor numbers. Increases in both cell death and premature cell cycle exit reduce the cortical precursor population. Moreover, the decrease of neuronal progenitors in *Cdk5rap2^{an/an}* animals correlates, paradoxically, with an increased mitotic index, suggesting delays in mitotic progression. We found altered mitotic orientation as well as increased abnormal mitotic figures, with aneupolar spindles, implicating essential roles for Cdk5rap2 in

spindle and centrosome function during neurogenesis. These data suggest that *CDK5RAP2* mutations in humans could cause microcephaly by mechanisms that include not only mitotic arrest and cell death, but also may include defects in cell fate determination. It is puzzling that anemia has not been reported in the few known human patients with *CDK5RAP2* mutations, as it is the defining feature of *Cdk5rap2^{an/an}* mutants. However, both the microcephaly and anemia in *Cdk5rap2^{an/an}* mice are variable and strain dependent, and so similar modifiers might affect penetrance in humans.

Mitotic defects have been previously associated with cell fate changes (Buchman and Tsai, 2007). It has been proposed that dividing VZ progenitors with vertical cleavage planes could

generate daughter cells with similar cell fates, and that small deviations from the vertical cleavage plane might be enough to disrupt these 'symmetric' cell divisions and reduce the progenitor population (Zhong and Chia, 2008). The 2-fold increase in cleavage planes parallel to the VS in *Cdk5rap2*[an/an] mice would reduce such symmetric cell divisions and might correlate with reduced progenitor numbers. RNAi knockdown experiments have also provided evidence that *Aspm*, another gene associated with microcephaly in humans, regulates mitotic spindle orientation and cell fate in early neurogenesis in mice (Fish et al., 2006). Furthermore, *Nde1* mutants have increased cell divisions with horizontal cleavage planes that correlate with premature depletion of the progenitor pool (Feng and Walsh, 2004). In these mutants, the decreased progenitor population correlates with premature and excessive generation of deep layer neurons, resulting in a larger fraction of cells leaving the cell cycle (Caviness et al., 2003). Although failure to maintain mitotic fidelity also increases the 'exit fraction' in *Cdk5rap2*[an/an] animals, unlike *Nde1* mutants, *Cdk5rap2*[an/an] mice show only modestly increased ratios of deeper versus superficial layer neurons. Lack of apparent overgeneration of deeper layer neurons in *Cdk5rap2*[an/an] embryos could result from increased cell death early in development, in contrast to *Nde1* mutants that show only modestly increased numbers of apoptotic cells (Feng and Walsh, 2004). Increased cell death in E10.5 *Cdk5rap2*[an/an] embryos correlates with a decrease in S-phase cells, suggesting that before neurogenic divisions start, Cdk5rap2 regulates the expansion of the progenitor pool. Moreover, the distribution of caspase 3-labeled cells and their co-immunoreactivity with either neuronal or progenitor markers in E12.5 *Cdk5rap2*[an/an] animals suggest that an overall increase in apoptosis affects both neurons and progenitors. In summary, changes in mitotic spindle orientation and premature cell cycle exit in *Cdk5rap2*[an/an] animals seem to correlate with cell fate determination defects; however, the dramatic increase in apoptosis might mask the premature and excessive generation of neurons, an expected outcome of faulty cell fate determination.

Cdk5rap2[an/an] mutants showed preferential thinning of the superficial neuronal layers. In evolutionary terms, these later-born neuronal layers only appeared after mammals diverged from reptiles (Nieuwenhuys, 1994), and the elaboration of the superficial layers has been proposed to be primarily responsible for the disproportionate expansion of the cerebral cortex relative to body size in mammals (Cheung et al., 2007). The evolutionary increase of superficial layers in mammals correlates with expansion of the SVZ, caused by increased basal progenitor numbers (Martinez-Cerdeno et al., 2006; Striedter and Charvet, 2009). In *Cdk5rap2*[an/an] animals, the reduction of Tbr2-immunoreactive progenitors could account, in part, for the diminished superficial layers. This is interesting because the *CDK5RAP2* gene shows a modest excess of non-conservative amino acid changes in the primate lineage leading to humans, suggesting that it might have been a target of evolution in primates (Evans et al., 2006). Thus, the essential roles of Cdk5rap2 in progenitor proliferation might reflect its relevance to the evolutionary expansion of the cerebral cortex (Kriegstein et al., 2006).

Cdk5rap2 contains a γ-tubulin-association domain that is found in other centrosomal proteins, including several in which mutations alter cell polarity, nuclear positioning, chromosomal alignment, spindle orientation and/or cleavage site specification (Megraw et al., 1999; Vaizel-Ohayon and Schejter, 1999; Venkatram et al., 2004; Verde et al., 2001). Cdk5rap2 and its fly ortholog Cnn

(Centrosomin) recruit the γ-TuRC to the centrosome (Fong et al., 2008; Heuer et al., 1995; Zhang and Megraw, 2007; Zheng et al., 1998). The primary role of the γ-TuRC is the nucleation of microtubules (Zheng et al., 1998). However, mounting evidence suggests additional roles during cell cycle progression for γ-tubulin and other γ-TuRC subunits. When γ-tubulin fails to localize to the centrosome, some cells arrest at G2–M, followed by apoptosis, whereas cells that bypass the G2–M arrest show highly defective mitoses with increased monopolar spindles (Zimmerman et al., 2004). Furthermore, in *Aspergillius nidulans*, the absence of γ-tubulin arrests cells at the metaphase-to-anaphase transition (Prigozhina et al., 2004). Interestingly, in-frame deletion of exon 4 in the *Cdk5rap2*[an] allele disrupts its γ-tubulin-association domain (Fong et al., 2008), and γ-tubulin localization to the centrosome appears decreased in *Cdk5rap2*[an/an] mouse embryonic fibroblasts (S.P.M. and M.D.F., unpublished). Therefore, interaction of Cdk5rap2 and γ-tubulin might be required to maintain mitotic fidelity in neuronal progenitors, as has been described in other tissues (Eppig and Barker, 1984).

The abnormal number of spindle poles and consequent aneuploidy in *Cdk5rap2*[an/an] mice might reflect defects in centrosome maturation or duplication. Centrosomes that fail to mature are less stable and prone to undergo splitting during mitosis (Fukasawa, 2007). Knockdown of CDK5RAP2 in interphase somatic cells causes abnormal centrosome splitting (Graser et al., 2007), suggesting defective centrosome maturation. Thus, failure of centrosome maturation followed by abnormal centrosome splitting would be an appealing mechanism to explain the aneupolar spindle poles observed in *Cdk5rap2*[an/an] neuronal progenitors. Alternatively, defects in centrosome duplication could also cause abnormal numbers of spindle poles (Fukasawa, 2007). In both cases, the abnormal number of centrosomes might produce abnormal mitosis that would either result in cell death or cell cycle arrest, as we have shown in *Cdk5rap2*[an/an] cortical progenitors. Alternatively, failure to arrest or exit the cell cycle might produce aneuploidy in *Cdk5rap2*[an/an] embryonic germ cells (Eppig and Barker, 1984) and, potentially, in neuronal precursors.

In mammals, an emerging hypothesis suggests that the asymmetric inheritance of the mother and daughter centrosomes (by the progenitor and neuronal daughter cells, respectively) is important for stem cell renewal during neurogenesis (Wang et al., 2009). In mice, the removal of ninein, a component of the mother centriole appendages, disrupts centrosome maturation and impairs centrosome asymmetric inheritance, resulting in neuronal overproduction due to altered cell fate (Wang et al., 2009). Interestingly, mutations in *Drosophila cnn* randomize centrosome asymmetric inheritance and affect germ cell fate determination (Yamashita et al., 2007). We hypothesize that because *Cdk5rap2*[an/an] animals have defects in mitotic orientation, the normal localization of centrosomes might be disrupted and could cause abnormal inheritance of the 'maternal' centrosome. Alternatively, disruption of Cdk5rap2-dependent steps of centrosome maturation could impair asymmetric centrosome inheritance in *Cdk5rap2*[an/an] mice. Either of these two mechanisms could then contribute to the premature depletion of the neuronal progenitor pool. A similar exhaustion of self-renewing progenitors might contribute to the hematological defects that originally defined the *Hertwig's anemia* mutation. Further analysis of centrosome maturation, duplication and inheritance in the absence of Cdk5rap2 might provide important additional insight into the relationship of the centrosome to cell fate determination and the pathology of microcephaly.

References

Angevine, J. B., Jr and Sidman, R. L. (1961). Autoradiographic study of cell migration during histogenesis of cerebral cortex in the mouse. *Nature* **192**, 766-768.

Baelde, H. J., Cleton-Jansen, A. M., van Beerendonk, H., Namba, M., Bovee, J. V. and Hogendoorn, P. C. (2001). High quality RNA isolation from tumours with low cellularity and high extracellular matrix component for cDNA microarrays: application to chondrosarcoma. *J. Clin. Pathol.* **54**, 778-782.

Bani-Yaghoub, M., Tremblay, R. G., Lei, J. X., Zhang, D., Zurakowski, B., Sandhu, J. K., Smith, B., Ribecco-Lutkiewicz, M., Kennedy, J., Walker, P. R. et al. (2006). Role of Sox2 in the development of the mouse neocortex. *Dev. Biol.* **295**, 52-66.

Barker, J. E. and Bernstein, S. E. (1983). Hertwig's anemia: characterization of the stem cell defect. *Blood* **61**, 765-769.

Barker, J. E., Deveau, S. A., Compton, S. T., Fancher, K. and Eppig, J. T. (2005). High incidence, early onset of histiocytic sarcomas in mice with Hertwig's anemia. *Exp. Hematol.* **33**, 1118-1129.

Bond, J., Roberts, E., Mochida, G. H., Hampshire, D. J., Scott, S., Askham, J. M., Springell, K., Mahadevan, M., Crow, Y. J., Markham, A. F. et al. (2002). ASPM is a major determinant of cerebral cortical size. *Nat. Genet.* **32**, 316-320.

Bond, J., Roberts, E., Springell, K., Lizarraga, S. B., Scott, S., Higgins, J., Hampshire, D. J., Morrison, E. E., Leal, G. F., Silva, E. O. et al. (2005). A centrosomal mechanism involving CDK5RAP2 and CENPJ controls brain size. *Nat. Genet.* **37**, 353-355.

Buchman, J. J. and Tsai, L. H. (2007). Spindle regulation in neural precursors of flies and mammals. *Nat. Rev. Neurosci.* **8**, 89-100.

Bultje, R. S., Castaneda-Castellanos, D. R., Jan, L. Y., Jan, Y. N., Kriegstein, A. R. and Shi, S. H. (2009). Mammalian Par3 regulates progenitor cell asymmetric division via notch signaling in the developing neocortex. *Neuron* **63**, 189-202.

Caviness, V. S., Jr, Goto, T., Tarui, T., Takahashi, T., Bhide, P. G. and Nowakowski, R. S. (2003). Cell output, cell cycle duration and neuronal specification: a model of integrated mechanisms of the neocortical proliferative process. *Cereb. Cortex* **13**, 592-598.

Chenn, A. and McConnell, S. K. (1995). Cleavage orientation and the asymmetric inheritance of Notch1 immunoreactivity in mammalian neurogenesis. *Cell* **82**, 631-641.

Chenn, A. and Walsh, C. A. (2002). Regulation of cerebral cortical size by control of cell cycle exit in neural precursors. *Science* **297**, 365-369.

Cheung, A. F., Pollen, A. A., Tavare, A., DeProto, J. and Molnar, Z. (2007). Comparative aspects of cortical neurogenesis in vertebrates. *J. Anat.* **211**, 164-176.

Ching, Y. P., Qi, Z. and Wang, J. H. (2000). Cloning of three novel neuronal Cdk5 activator binding proteins. *Gene* **242**, 285-294.

Englund, C., Fink, A., Lau, C., Pham, D., Daza, R. A., Bulfone, A., Kowalczyk, T. and Hevner, R. F. (2005). Pax6, Tbr2, and Tbr1 are expressed sequentially by radial glia, intermediate progenitor cells, and postmitotic neurons in developing neocortex. *J. Neurosci.* **25**, 247-251.

Eppig, J. T. and Barker, J. E. (1984). Chromosome abnormalities in mice with Hertwig's anemia. *Blood* **64**, 727-732.

Eppig, J. T. and Barker, J. E. (1989). Deleterious effects of irradiation and bone marrow transplantation therapy in the genetically anemic an/an mouse. *Blood* **73**, 1373-1379.

Evans, P. D., Vallender, E. J. and Lahn, B. T. (2006). Molecular evolution of the brain size regulator genes CDK5RAP2 and CENPJ. *Gene* **375**, 75-79.

Feng, Y. and Walsh, C. A. (2004). Mitotic spindle regulation by Nde1 controls cerebral cortical size. *Neuron* **44**, 279-293.

Ferland, R. J., Cherry, T. J., Preware, P. O., Morrisey, E. E. and Walsh, C. A. (2003). Characterization of Foxp2 and Foxp1 mRNA and protein in the developing and mature brain. *J. Comp. Neurol.* **460**, 266-279.

Fish, J. L., Kosodo, Y., Enard, W., Paabo, S. and Huttner, W. B. (2006). Aspm specifically maintains symmetric proliferative divisions of neuroepithelial cells. *Proc. Natl. Acad. Sci. USA* **103**, 10438-10443.

Fong, K. W., Choi, Y. K., Rattner, J. B. and Qi, R. Z. (2008). CDK5RAP2 is a pericentriolar protein that functions in centrosomal attachment of the {gamma}-tubulin ring complex. *Mol. Biol. Cell* **19**, 115-125.

Fukasawa, K. (2007). Oncogenes and tumour suppressors take on centrosomes. *Nat. Rev. Cancer* **7**, 911-924.

Gleeson, J. G., Lin, P. T., Flanagan, L. A. and Walsh, C. A. (1999). Doublecortin is a microtubule-associated protein and is expressed widely by migrating neurons. *Neuron* **23**, 257-271.

Gotz, M. and Huttner, W. B. (2005). The cell biology of neurogenesis. *Nat. Rev. Mol. Cell Biol.* **6**, 777-788.

Graser, S., Stierhof, Y. D. and Nigg, E. A. (2007). Cep68 and Cep215 (Cdk5rap2) are required for centrosome cohesion. *J. Cell Sci.* **120**, 4321-4331.

Haydar, T. F., Ang, E., Jr and Rakic, P. (2003). Mitotic spindle rotation and mode of cell division in the developing telencephalon. *Proc. Natl. Acad. Sci. USA* **100**, 2890-2895.

Hertwig, P. (1942). Neue Mutationen und Koppelungsgruppen bei der Hausmaus. *Z. Indukt. Abstamm. Vererbungsl.* **80**, 220-246.

Heuer, J. G., Li, K. and Kaufman, T. C. (1995). The Drosophila homeotic target gene centrosomin (cnn) encodes a novel centrosomal protein with leucine zippers and maps to a genomic region required for midgut morphogenesis. *Development* **121**, 3861-3876.

Hevner, R. F., Shi, L., Justice, N., Hsueh, Y., Sheng, M., Smiga, S., Bulfone, A., Goffinet, A. M., Campagnoni, A. T. and Rubenstein, J. L. (2001). Tbr1 regulates differentiation of the preplate and layer 6. *Neuron* **29**, 353-366.

Higginbotham, H. R. and Gleeson, J. G. (2007). The centrosome in neuronal development. *Trends Neurosci.* **30**, 276-283.

Katayama, H., Brinkley, W. R. and Sen, S. (2003). The Aurora kinases: role in cell transformation and tumorigenesis. *Cancer Metastasis Rev.* **22**, 451-464.

Kriegstein, A., Noctor, S. and Martinez-Cerdeno, V. (2006). Patterns of neural stem and progenitor cell division may underlie evolutionary cortical expansion. *Nat. Rev. Neurosci.* **7**, 883-890.

Lee, L., DeBono, C. A., Campagna, D. R., Young, D. C., Moody, D. B. and Fleming, M. D. (2007). Loss of the acyl-CoA binding protein (Acbp) results in fatty acid metabolism abnormalities in mouse hair and skin. *J. Invest. Dermatol.* **127**, 16-23.

Leid, M., Ishmael, J. E., Avram, D., Shepherd, D., Fraulob, V. and Dolle, P. (2004). CTIP1 and CTIP2 are differentially expressed during mouse embryogenesis. *Gene Expr. Patterns* **4**, 733-739.

Martinez-Cerdeno, V., Noctor, S. C. and Kriegstein, A. R. (2006). The role of intermediate progenitor cells in the evolutionary expansion of the cerebral cortex. *Cereb. Cortex* **16 Suppl. 1**, i152-i161.

McEvilly, R. J., de Diaz, M. O., Schonemann, M. D., Hooshmand, F. and Rosenfeld, M. G. (2002). Transcriptional regulation of cortical neuron migration by POU domain factors. *Science* **295**, 1528-1532.

Megraw, T. L., Li, K., Kao, L. R. and Kaufman, T. C. (1999). The centrosomin protein is required for centrosome assembly and function during cleavage in Drosophila. *Development* **126**, 2829-2839.

Misson, J. P., Edwards, M. A., Yamamoto, M. and Caviness, V. S., Jr (1988). Identification of radial glial cells within the developing murine central nervous system: studies based upon a new immunohistochemical marker. *Brain Res. Dev. Brain Res.* **44**, 95-108.

Mochida, G. H. (2008). Molecular genetics of lissencephaly and microcephaly. *Brain Nerve* **60**, 437-444.

Nieto, M., Monuki, E. S., Tang, H., Imitola, J., Haubst, N., Khoury, S. J., Cunningham, J., Gotz, M. and Walsh, C. A. (2004). Expression of Cux-1 and Cux-2 in the subventricular zone and upper layers II-IV of the cerebral cortex. *J. Comp. Neurol.* **479**, 168-180.

Nieuwenhuys, R. (1994). The neocortex. An overview of its evolutionary development, structural organization and synaptology. *Anat. Embryol. (Berl.)* **190**, 307-337.

Noctor, S. C., Flint, A. C., Weissman, T. A., Dammerman, R. S. and Kriegstein, A. R. (2001). Neurons derived from radial glial cells establish radial units in neocortex. *Nature* **409**, 714-720.

Pontious, A., Kowalczyk, T., Englund, C. and Hevner, R. F. (2008). Role of intermediate progenitor cells in cerebral cortex development. *Dev. Neurosci.* **30**, 24-32.

Prigozhina, N. L., Oakley, C. E., Lewis, A. M., Nayak, T., Osmani, S. A. and Oakley, B. R. (2004). gamma-tubulin plays an essential role in the coordination of mitotic events. *Mol. Biol. Cell* **15**, 1374-1386.

Rakic, P. (1974). Neurons in rhesus monkey visual cortex: systematic relation between time of origin and eventual disposition. *Science* **183**, 425-427.

Rakic, P. (2009). Evolution of the neocortex: a perspective from developmental biology. *Nat. Rev. Neurosci.* **10**, 724-735.

Russell, E. S., McFarland, E. C. and Peters, H. (1985). Gametic and pleiotropic defects in mouse fetuses with Hertwig's macrocytic anemia. *Dev. Biol.* **110**, 331-337.

Sanada, K. and Tsai, L. H. (2005). G protein betagamma subunits and AGS3 control spindle orientation and asymmetric cell fate of cerebral cortical progenitors. *Cell* **122**, 119-131.

Sepp, K. J., Hong, P., Lizarraga, S. B., Liu, J. S., Mejia, L. A., Walsh, C. A. and Perrimon, N. (2008). Identification of neural outgrowth genes using genome-wide RNAi. *PLoS Genet.* **4**, e1000111.

Shibata, T., Yamada, K., Watanabe, M., Ikenaka, K., Wada, K., Tanaka, K. and Inoue, Y. (1997). Glutamate transporter GLAST is expressed in the radial glia-astrocyte lineage of developing mouse spinal cord. *J. Neurosci.* **17**, 9212-9219.

Striedter, G. F. and Charvet, C. J. (2009). Telencephalon enlargement by the convergent evolution of expanded subventricular zones. *Biol. Lett.* **5**, 134-137.

Vader, G. and Lens, S. M. (2008). The Aurora kinase family in cell division and cancer. *Biochim. Biophys. Acta* **1786**, 60-72.

Vaizel-Ohayon, D. and Schejter, E. D. (1999). Mutations in centrosomin reveal requirements for centrosomal function during early Drosophila embryogenesis. *Curr. Biol.* **9**, 889-898.

Venkatram, S., Tasto, J. J., Feoktistova, A., Jennings, J. L., Link, A. J. and Gould, K. L. (2004). Identification and characterization of two novel proteins affecting fission yeast gamma-tubulin complex function. *Mol. Biol. Cell* **15**, 2287-2301.

Verde, I., Pahlke, G., Salanova, M., Zhang, G., Wang, S., Coletti, D., Onuffer, J., Jin, S. L. and Conti, M. (2001). Myomegalin is a novel protein of the golgi/centrosome that interacts with a cyclic nucleotide phosphodiesterase. *J. Biol. Chem.* **276**, 11189-11198.

Wang, X., Tsai, J. W., Imai, J. H., Lian, W. N., Vallee, R. B. and Shi, S. H. (2009). Asymmetric centrosome inheritance maintains neural progenitors in the neocortex. *Nature* **461**, 947-955.

Woods, C. G., Bond, J. and Enard, W. (2005). Autosomal recessive primary microcephaly (MCPH): a review of clinical, molecular, and evolutionary findings. *Am. J. Hum. Genet.* **76**, 717-728.

Yamashita, Y. M., Mahowald, A. P., Perlin, J. R. and Fuller, M. T. (2007). Asymmetric inheritance of mother versus daughter centrosome in stem cell division. *Science* **315**, 518-521.

Yingling, J., Youn, Y. H., Darling, D., Toyo-Oka, K., Pramparo, T., Hirotsune, S. and Wynshaw-Boris, A. (2008). Neuroepithelial stem cell proliferation requires LIS1 for precise spindle orientation and symmetric division. *Cell* **132**, 474-486.

Zhang, J. and Megraw, T. L. (2007). Proper recruitment of gamma-tubulin and D-TACC/Msps to embryonic Drosophila centrosomes requires Centrosomin Motif 1. *Mol. Biol. Cell* **18**, 4037-4049.

Zheng, Y., Wong, M. L., Alberts, B. and Mitchison, T. (1998). Purification and assay of gamma tubulin ring complex. *Methods Enzymol.* **298**, 218-228.

Zhong, W. and Chia, W. (2008). Neurogenesis and asymmetric cell division. *Curr. Opin. Neurobiol.* **18**, 4-11.

Zimmerman, W. C., Sillibourne, J., Rosa, J. and Doxsey, S. J. (2004). Mitosis-specific anchoring of gamma tubulin complexes by pericentrin controls spindle organization and mitotic entry. *Mol. Biol. Cell* **15**, 3642-3657.